euspen's 22nd International Conference & Exhibition, Geneva, CH, May/June 2022
www.euspen.eu

# A novel approach for geometrical deviations determination of lattice structures from volumetric data

Marc-Antoine de Pastre[1], Yann Quinsat[1]

[1]*LURPA, ENS Paris-Saclay, Université Paris-Saclay, 91190 Gif-sur-Yvette, France*

*marc-antoine.de_pastre@ens-paris-saclay.fr*

**Abstract**
Additive manufacturing (AM) questions traditional approaches that manufacturer and metrologist have developed relative to formative or subtractive manufacturing technologies. As specific-to-AM parts, lattice structures are being investigated in many applications and efforts are focussed on modelling manufactured different-scale defects to predict the part properties before manufacturing. To date, X-ray computed tomography (XCT) is the most suited measuring instrument to reveal additively manufactured part internal defects, i.e. defects inaccessible to optical or tactile instruments. However, XCT requires surface determination tools which choice may be discussed. In this paper, a virtual volume correlation (V2C) method is proposed relying on modal decomposition. In other words, lattice structure shape defects are expressed directly from volumetric data, without any use of XCT surface determination tool. Extending previous works validated for representative lattice struts, entire lattice structure shape defect is identified by iteratively deforming a virtual volume, to minimise its least square grey level differences towards the measured volume. The proposed method particularly describes the strut form defects and the node displacements. This method allows to define at the same time and separately the shape defect of each strut but also the global geometrical defect of the structure. This approach is more relevant to assess the suitability of the structure with respect to mechanical loads than a deviation map that is difficult to handle.

Computed tomography, lattice structures, virtual volume correlation, modal decomposition

## 1. Introduction

Additively manufactured lattice structures are challenging to measure [1, 2]. They involve 3-dimensional repeated patterns where all surfaces are not accessible to traditional optical or tactical measuring systems. Alternatively, X-ray computed tomography (XCT) has the noteworthy advantage of being able to measure both internal and external part surfaces [2, 3]. Measurement by XCT has three main steps: the measurement itself by projecting X-rays, reconstruction and surface determination. Whereas reconstruction is mainly performed by filtered backprojection algorithms, surface determination depends on the user's choice such as ISO or gradient-based methods [4, 5].

In literature, previous work has compared surface determination tools [4, 6, 7]. Although ISO methods are easy to understand and to implement, gradient-based tools are mainly commercial software black boxes, where parameters can't be easily checked. That is why, there is no definitive solution about surface determination tools and discussions are still ongoing. To overcome this surface determination tool uncertainty, we propose a novel approach to estimate lattice structure geometrical deviations based on virtual volume correlation (V2C). This paper particularly extends previous work [8], validated for elementary struts representative of a BCCz lattice structure, to the entire lattice structure, in order to identify its geometrical deviations. V2C adaptation is presented in section 2 and applied on a substructure extracted from a 2x2x2 BCCz lattice structure in section 3.

## 2. Methodology

### *2.1. Virtual volume correlation for lattice structure*

V2C consists of identifying the displacement field embedded in measured volumetric data [8]. This is done by successively deforming a virtual volume until it matches the measured volume, which is achieved by minimising the grey level difference between both volumes. This section presents the V2C suited for an entire lattice structure through the description of an unit BCCz cell (see Figure 1) that is repeated in three directions to form the net. An unit cell is composed of struts and a strut indexed by p is defined by two nodes: $N_i^p$ and $N_j^p$.

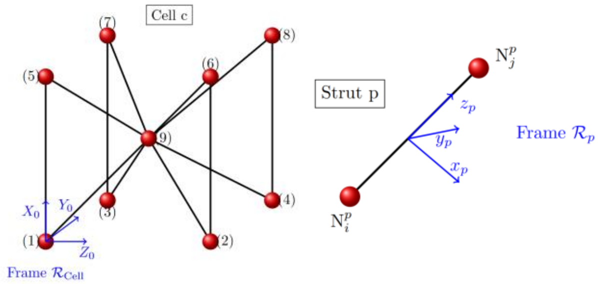


**Figure 1.** Cell (left) and strut (right) wire representation with associated frames

The V2C problem can be expressed by the following correlation score minimisation:

$$\Phi(\mathbf{u}) = \iiint_{ROI} [f(\mathbf{X}) - g(\mathbf{X} + \mathbf{u})]^2 \, d\Omega \tag{1}$$

Where $f$ and $g$ refer respectively to the physical (stemming from XCT measurement) and virtual (numerically computed) volumes.

$ROI$ is the region of interest of the measured volume and $\mathbf{u}$ refers to the displacement field that should be identified.

As the structure is made of p struts, the problem can be decomposed into p correlation problems with limit conditions on the node displacements. We focussed the correlation on struts rather than on nodes. In fact, node identification from volumetric data is challenging as the structure manufacturing itself introduces fillets and increases the node position determination uncertainty.

The V2C problem can then be written as:

$$\begin{cases} \text{Correlation score that should be minimised :} \\ \Phi(\mathbf{u}) = \sum_{p=1}^{N_{struts}} \iiint_{ROI_p} \left[ f(\mathbf{X}) - g\left(\mathbf{X} + \mathbf{u}_{p|\mathcal{R}_{cell}}\right)\right]^2 d\Omega \quad (2) \\ \underline{\text{Limit conditions:}} \text{ common nodes to several struts should have the same displacement.} \end{cases}$$

where $N_{struts}$ is the number of struts, $ROI_p$ is the region of interest defined for the p strut. $\mathbf{u}_{p|\mathcal{R}_{cell}}$ refers to the displacement field applied to the p strut relative to the cell frame. More details are provided in the next section.

### 2.2. Shape defect basis

For lattice cells, the question of whether geometric deviations are studied on the strut scale or on the entire structure should be raised. In this approach, we propose to combine both scales by simultaneously studying struts shape defects and the overall geometric deviations of the structure.
In the following equation, the displacement field is assumed to be found by modal decomposition [8, 9]. More precisely:

$$\mathbf{u}_{p|\mathcal{R}_{cell}} = \sum_k \lambda_k^p \mathbf{u}_{k|\mathcal{R}_{cell}}^{\mathrm{p}} = \sum_k \lambda_k^p \mathcal{T}_{\mathcal{R}_\mathrm{p} \to \mathcal{R}_{cell}} \mathbf{u}_{k|\mathcal{R}_p}^{\mathrm{p}} \quad (3)$$

where $\lambda_k^p$ are the components of $\{\boldsymbol{\lambda}^p\}$ and refer to the modal amplitude associated with the considered modes of the p strut, $\mathcal{T}_{\mathcal{R}_p \to \mathcal{R}_{cell}}$ refers to the geometric frame transformation matrix between $\mathcal{R}_p$ and $\mathcal{R}_{cell}$ frames.
In the following, modes are defined by family types:

- Rigid transformations of the struts (3 translations and 2 rotations)
- Dilatation of strut diameter
- Vertical defects along the struts
- Plane defects described by sinusoidal descriptors.

All these modes define the considered shape defect basis which can be adapted for each strut. The suitability of this shape defect basis towards cylindrical shapes has been discussed in [8, 9] and and a literature review on the modelling of shape defects is proposed in [8].

$\{\boldsymbol{\lambda}^p\}$ are found by minimisation of the correlation score reduced to the p strut and equation 2 can be expressed as:

$$\begin{cases} \text{Correlation score minimisation:} \\ \{\boldsymbol{\lambda}_{min}^{\boldsymbol{p}}\} = \underset{\boldsymbol{\lambda}^{\boldsymbol{p}}}{argmin}\ \Phi_\mathrm{p}(\boldsymbol{u}) \quad (4) \\ \underline{\text{Limit conditions:}} \text{ common nodes to several struts should have the same displacement.} \end{cases}$$

A first order linearisation and the application of a Gauss-Newton optimisation scheme [8] leads to:

$$\begin{cases} \boldsymbol{M}^p \boldsymbol{\Delta\lambda}^p = \boldsymbol{b}^p \quad (5) \\ \underline{\text{Limit conditions:}} \text{ common nodes to several struts should have the same displacement.} \end{cases}$$

with $\boldsymbol{\Delta\lambda}^p$ the elementary modal amplitude to apply to the p strut. This iterative scheme is repeated until convergence.

### 2.3. Association of struts

By developing equations and taking into consideration the limit conditions, the correlation problem is transposed from the $\mathcal{R}_p$ frame to the $\mathcal{R}_{cell}$ frame by application of a variable transformation matrix $\boldsymbol{Q}$ (see equation 6). In other words, rigid transformations expressed in the local strut frame are then translated into nodal displacements in the cell frame. This allows the expression of the minimisation problem for all struts in a row and the integration of limit conditions in the problem expression.

With $\{\boldsymbol{\lambda}\}_{p=\{1,\ldots,N_{struts}\}}$ being the concatenated list of all $\{\boldsymbol{\lambda}^p\}$ defined for all p struts, then the variable transformation is expressed as:

$$\{\boldsymbol{\lambda}\} = \boldsymbol{Q}\,\{\boldsymbol{\lambda}^*\} \quad (6)$$

where $\{\boldsymbol{\lambda}^*\}$ is the list of all nodal amplitudes expressed in the $\mathcal{R}_{cell}$ frame concatenated with non-rigid modal amplitudes for all struts. By integrating limit conditions, and applying equation 6 to elementary displacement, equation 5 is then simplified to:

$$(\boldsymbol{Q}^T \boldsymbol{M} \boldsymbol{Q}) \boldsymbol{\Delta\lambda}^* = \boldsymbol{Q}^T \boldsymbol{b} \quad (7)$$

thus,

$$\boldsymbol{\Delta\lambda} = \boldsymbol{Q}[(\boldsymbol{Q}^T \boldsymbol{M} \boldsymbol{Q})^{-1} (\boldsymbol{Q}^T \boldsymbol{b})] \quad (8)$$

with $\boldsymbol{\Delta\lambda}$ being the elementary modal amplitudes to apply to all struts, resulting in an iteratively updated virtual volume. The described method can now be applied on a manufactured lattice sample.

### 2.3. Sample manufacturing and measurement

The sample is a 2x2x2 BCCz lattice structure where the beam radii have been set to 0.6 mm and struts have a 6 mm length, all designed in a computer-aided-design (CAD) software. The lattice structure was produced by laser powder bed fusion (PBF) on an Addup FormUp 350 using Inconel 718 powder and the printing parameters displayed in Table 1.

**Table 1.** Printing parameters

| | |
|---|---|
| **Powder** | Inconel 718 |
| **Layer thickness** | 40 µm |
| **Laser power** | 220 W |
| **Scan speed** | 2100 mm.s$^{-1}$ |
| **Contour scan power** | 210 W |
| **Contour scan speed** | 1800 mm.s$^{-1}$ |
| **Hatch space** | 55 µm |

The manufactured sample was washed with water and dried with compressed air. It was removed from the substrate using an electrical discharge machine.

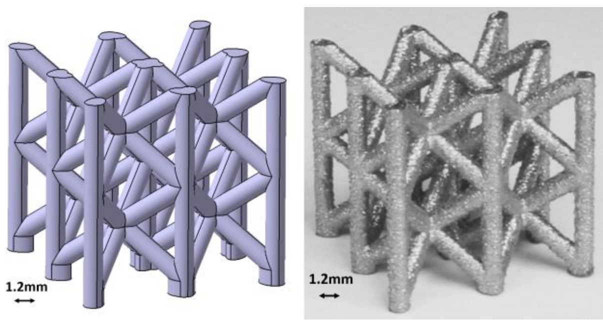


**Figure 2.** Designed (left) and manufactured (right) 2x2x2 lattice structure

The manufactured lattice structure was then measured using XCT with the measurement setups summarised in Table 2:

**Table 2.** XCT measurement setups

| | |
|---|---|
| **Magnification** | x11.4% |
| **Voxel size** | 15 µm |
| **Projections** | 1200 |
| **Tube voltage** | 180 kV |
| **Tube current** | 130 µA |

A warmup scan of approximately 30 minutes was performed prior to the scan and data were reconstructed in the manufacturer's software, using a filtered backprojection algorithm and a beam hardening correction without specific filter. Reconstruction was saved in a .raw file format. An elementary 1x1x1 substructure was extracted from the 2x2x2 measured volumetric data; this was done to reduce the computation time and the size of data handled in this problem.

### *2.4. Numeric methodology*

V2C was applied on the measured substructure, resulting in a V2C envelope. Vertical defects were taken as simple flexion, and plane defects were assigned to 10 sinusoidal modes. At the same time, $ISO_{50\%}$ [4] envelope was extracted from the substructure volumetric data. Each envelope was compared to the CAD model, and was then compared to one another. All data treatments included in this paper are summarised in the pipeline displayed in Figure 3.

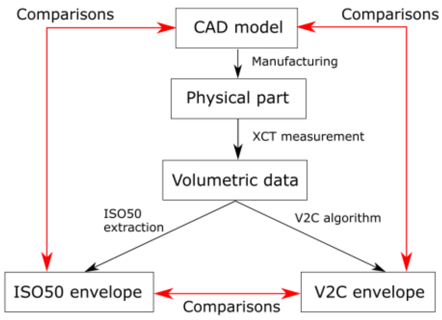


**Figure 3.** Data treatment pipeline

### 3. Results

Nodal displacement field was identified by V2C and is shown by each blue array in Figure 4. Associated nodal displacement norms are displayed in Figure 5. It is worth noting that V2C independently corrects nodal positions resulting in the nominal model deformation, or the structure shape defect identification.

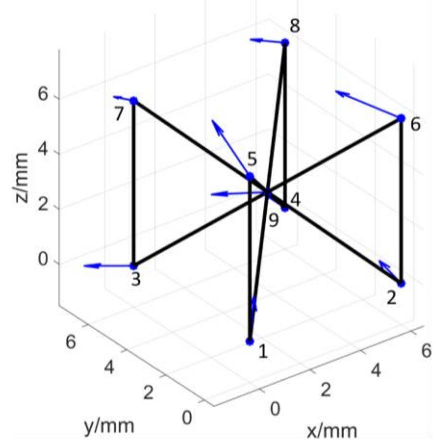


**Figure 4.** Nodal displacement vectors identified by V2C, represented on the lattice wire model. Vector amplitudes have been enhanced for more readability. Dilatation, plane and vertical defects are not represented.

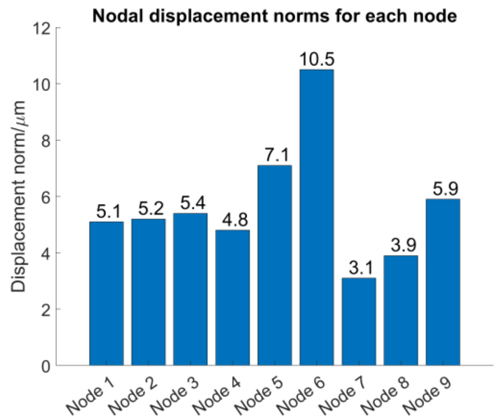


**Figure 5.** Nodal displacement norms.

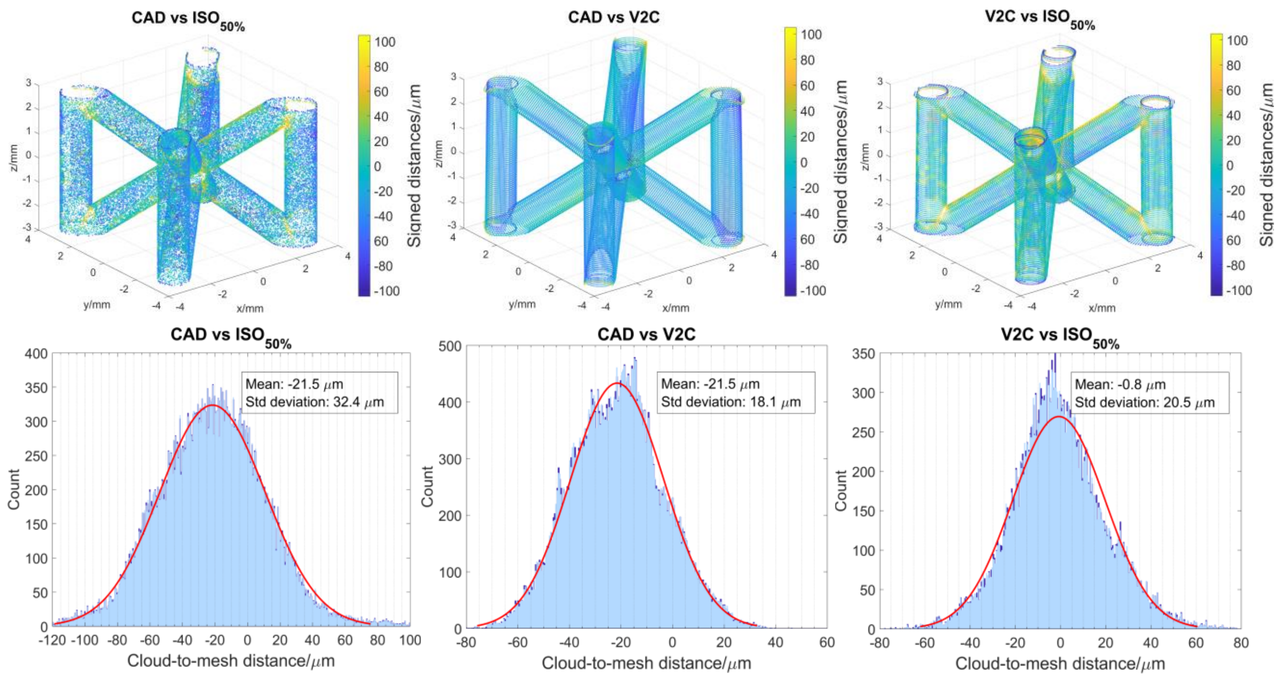


**Figure 6.** Signed distances between comparative sets: CAD model vs $ISO_{50\%}$ envelope (left), CAD vs V2C (middle) and V2C vs $ISO_{50\%}$ (right)

Figure 6 displays signed distances between described comparative sets. Distance distributions are shown in a histogram layout and a Gaussian normal distribution fitting was applied on the data. Distances near the lattice nodes were excluded from the histogram plots to avoid fillet fitting effects. To refine the analysis of the data distributions, statistical boxplots of the distributions are displayed in Figure 7 for each of the considered comparative sets.

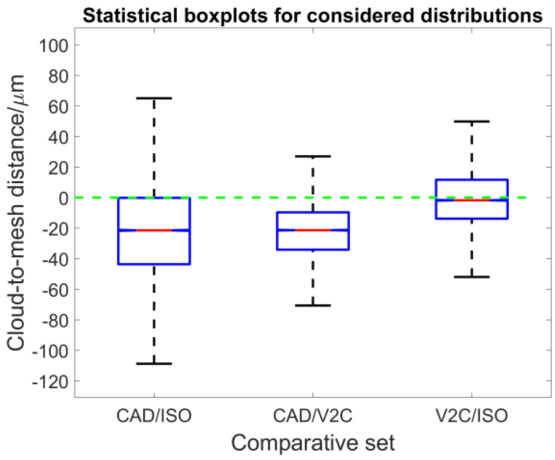


**Figure 7.** Statistical boxplots for considered comparative sets (green dashed line highlights the 0 value).

## 4. Discussion

When compared to the CAD model, $ISO_{50\%}$ and V2C envelopes provide similar results in terms of mean values around -21 µm (see Figure 6 and 7). This negative mean value may be explained by an overall material retraction during manufacturing. Standard deviation discrepancies are explained by the $ISO_{50\%}$ envelope embedding surface roughness which is not estimated by the V2C algorithm. As a result, the CAD/V2C distribution is narrower than the CAD/$ISO_{50\%}$ set. In addition, relative to the chosen shape defect basis (see section 2.2), V2C provides shape defect information and is not sensible to lower defect wavelengths. A similar observation is made in Figure 7 with CAD/V2C set showing a narrower distribution width than the CAD/$ISO_{50\%}$ set. The V2C/$ISO_{50\%}$ comparative set shows that apart from the roughness consideration, V2C and $ISO_{50\%}$ have common trends. As illustrated in both Figures 6 and 7, the centred V2C/$ISO_{50\%}$ set mean value confirms that V2C is efficient in estimating the structure shape defect relative to the considered basis.

In Figure 6, signed distance plots also show that identifying nodes in a lattice structure is a challenging task when fillets between struts are introduced at the manufacturing step. Indeed, these regions have the highest discrepancies in all of the considered comparative sets. Thus, focussing on struts allows access to all the information embedded in the volumetric data rather than adding node determination and approximation steps. This choice provides an overall estimation of both orientation and deformation defects of each strut composing of the lattice structure, with node connections defined as limit conditions.

A note should be made about the resulting modal decomposition amplitude for the lattice structure. Considering the nature of the strut i.e. vertical or inclinded, modal amplitudes are similar to the modal amplitude obtained in the strut analysis performed in [8]. In other words, modal amplitude computed in this study are in the same order as node displacement displayed in Figure 5.

## 5. Conclusion

This paper introduced the V2C method adapted to entire lattice structures. We show that V2C is a tool that can provide the CAD model with shape defect information. The main advantage of this virtual volume correlation technique is that it relies only on volumetric data, without any post-reconstruction additional step, in order to estimate lattice structure shape defects relative to a chosen shape defect basis. Previous work supports the suitability of the considered shape defect basis in this paper. Improvements to the basis could focus on introducing lower wavelength defects and integrating specific-to-the-process defects such as spatters or local recesses. The latter may require to turn the proposed approach into a mesh-based one to specifically address these typologies of defects. In addition, as V2C deals with volumetric data, V2C requires strong computation resources, notably RAM resources. As an illustration, this work required about 200 Gb of RAM. Future work will continue to focus on defining a strategy such as resolution adaptation, to apply V2C in a reasonable computation time.


**Acknowledgments** CT measurements at ENS Paris-Saclay have been financially supported by the French *Agence Nationale de la Recherche*, through the *Investissements d'avenir* program (ANR-10- EQPX-37 MATMECA Grant)

This work was performed using HPC resources from the *Mésocentre* computing center of CentraleSupélec and École Normale Supérieure Paris-Saclay supported by CNRS and Région Île-de-France (http://mesocentre.centralesupelec.fr/).


## References


[1] P. Sperling, A. du Plessis, and G. Schwaderer, "Challenges and approaches for metrology of additive manufactured lattice structures by industrial x-ray computed tomography," *Advanced Materials Research*, vol. **1161**, pp. 131–136, 03 2021

[2] I. Echeta, X. Feng, B. Dutton, S. Piano, and R. Leach, "Review of defects in lattice structures manufactured by powder bed fusion," *International Journal of Advanced Manufacturing Technology*, vol. **106**, 01 2020

[3] L. Chiffre, S. Carmignato, J.-P. Kruth, R. Schmitt, and A. Weckenmann, "Industrial applications of computed tomography," *CIRP Annals - Manufacturing Technology*, vol. **63**, 12 2014

[4] J. P. Kruth, M. Bartscher, S. Carmignato, R. Schmitt, L. De Chiffre, and A. Weckenmann, "Computed tomography for dimensional metrology," *CIRP annals*, vol. **60**, no. 2, pp. 821–842, 2011

[5] L. Ding and A. Goshtasby, "On the canny edge detector," *Pattern Recognition*, vol. **34**, no. 3, pp. 721–725, 2001

[6] S. Lou, W. Sun, W. Zeng, L. Pagani, X. Jiang, and P. Scott, "Development of 2d local searching algorithms for surface determination of x-ray computed tomography measurement," in 3rd Dimensional X-ray Computed Tomography Conference at University of Nottingham, 07 2018

[7] F. B. de Oliveira, A. Stolfi, M. Bartscher, L. De Chiffre, and U. Neuschaefer-Rube, "Experimental investigation of surface determination process on multi-material components for dimensional computed tomography," *Case studies in nondestructive testing and evaluation*, vol. **6**, pp. 93–103, 2016

[8] M.-A. de Pastre, Y. Quinsat, and C. Lartigue, "Shape defect analysis from volumetric data - application to lattice struts in additive manufacturing," *Precision Engineering*, vol. **76**, pp. 12–28, 2022

[9] L. Homri, E. Goka, G. Levasseur, and J.-Y. Dantan, "Tolerance analysis: Form defects modeling and simulation by modal decomposition and optimization," *Computer Aided Design*, vol. **91**, 06 2017